



Production and characterization of carbon/carbon composites from thermoplastic matrices

Luiza dos Santos Conejo^{1,2} · Hermes Rocha de Meneses Neto¹ · Juliana Bovi de Oliveira¹ · Luis Felipe de Paula Santos¹ · Roberto Zenhei Nakazato³ · Luis Rogerio de Oliveira Hein¹ · Winand Kok⁴ · Edson Cocchieri Botelho¹

Received: 9 September 2020 / Accepted: 1 February 2021 / Published online: 13 March 2021
© The Polymer Society, Taipei 2021

Abstract

Carbon-carbon composites (C/C) are those that have carbonaceous matrix reinforced with carbon fiber. They are widely used in the aerospace field, due mainly to the properties such as low density, high stiffness, and excellent thermal resistance, in comparison to the ones with polymer or metallic matrix. They are obtained through composites of polymer matrix (thermoset or thermoplastic), from the heat treatment of carbonization. The objective of this work is to produce the C/C composite material from three different thermoplastic laminates (PEKK/CF, PEEK/CF and LMPAEK/CF) as well as to compare these materials with C/C composites obtained from thermoset matrices, to show their advantages and disadvantages in relation to them. Such comparison was substantiated with TGA, DSC, SEM and XRD analyzes. In this work, the TGA showed the proposed process presents a lower mass loss, resulting in a faster and cheaper process, comparing thermoplastic with thermoset laminates. The DSC tests provided the basis for establishing the different heating rates. Through the SEM images it was possible to analyze the carbonization process. Finally, analyzes of cyclic voltammetry were made; through a comparison with Platinum electrode, C/C electrodes proved to be suitable for this application. Also, electrodes obtained from PEEK/CF presented better electrochemical responses.

Keywords Carbon/carbon composites · Thermoplastic matrix · Thermal analyses

Introduction

Composite materials have been widely used in different industrial sectors, such as in the aeronautical [1], aerospace [2], automobile [3], electronics [4], medical [5], among others. Within this very broad area are the Carbon/Carbon composites (C/C) considered an advanced thermostructural material is currently used, especially in aerospace applications, due to its low density, good thermal resistance

and rigidity, low coefficient of thermal expansion [6, 7]. By definition, the carbonaceous matrix that constitutes this material comes from a polymer with high carbon content in its formulation and can be obtained through carbonization process. This process is a thermal treatment that occurs at least under 1000°C with an inert atmosphere, in order to eliminate all the volatile present in the composites, specifically of the polymeric matrix, to remain only the carbon element. The carbonaceous reinforcement generally used is carbon fiber, which in its fundamental state is already constituted only by the carbon element. The differences between the carbon bonds help to explain the different behaviors that the carbon element has in the same composite, acting simultaneously as matrix and reinforcement [8–12].

Currently most of the works involving carbon/carbon composites use thermoset matrices, considering the high content of carbon present in their chains [13]. The properties of this material are influenced by several factors including density, type of carbon fiber, matrix/reinforcement interface, matrix microstructure, and porosity. Normally, after

✉ Edson Cocchieri Botelho
edson.cocchieri.botelho@gmail.com

¹ Department of Materials and Technology, São Paulo State University, UNESP, Guaratinguetá, São Paulo, Brazil

² Lightweight Structures Laboratory, Institute for Technological Research (IPT), São José dos Campos, Brazil

³ Department of Physics and Chemistry, São Paulo State University, UNESP, Guaratinguetá, São Paulo, Brazil

⁴ Toray Advanced Composites, Nijverdal, Netherlands

carbonization the materials have pores that impair the material's properties, limiting its application [14]. Hence to correct this, the impregnation process is performed, where the pores in the C/C composite after carbonization are filled by the same resin used in the processing of the original composite, and then the carbonization process is performed again. Several re-impregnations may be performed until an acceptable number of pores is obtained in the final composite, which may vary according to the application.

For the C/C composites obtained through thermoplastic matrix composites, the impregnation process also occurs, but it is expected that a smaller number of re-impregnations is required, considering that there is a minor weight loss throughout the carbonization processes. Therefore, would make the process cheaper, considering the lower expenditure of material for re-impregnation, as well as hours in the furnace, and from the economic point of view, obtaining C/C composites from thermoplastic matrix composites is quite feasible.

Taking this into account, this work seeks to obtain C/C composites from the use of thermoplastic polymers, that have high carbon content in their matrices, such as PEEK/CF (Poly(ether-ether-ketone) reinforced with Carbon Fibers), LMPAEK/CF (Low Melting Poly(aryl-ether-ketone) reinforced with Carbon Fibers) and PEKK/CF (Poly(ether-ketone-ketone) reinforced with Carbon Fibers). About the matrices used in this work, the PEEK is a high-performance thermoplastic, and it stands out for its high crystallinity, excellent mechanical resistance, and chemical stability. In addition, it has a glass transition and melting temperature around 143°C and 343°C, respectively. Due to the high resistance to chemical products and hydrolysis up to 260°C, as well as good tribological, and electrical properties, PEEK is applied in almost all branches of industry [15, 16]. Figure 1 shows the chemical structure of PEEK. It is noteworthy that all the polymers studied in this work are from the same "family", the PAEK (Poly(aryl-ether-ketone)) and present a similar chemical structure to that depicted in Fig. 1.

The PEKK has been receiving a lot of attention in the last years, mainly of the aeronautical industry, due to characteristics such as high values of glass transition temperature (156°C) [17, 18], mechanical strength and modulus of elasticity, low moisture absorption, excellent

resistance to variations in climatic conditions, combined with a relatively low specific weight, and high stiffness [17, 19]. Finally, LMPAEK has an excellent combination of properties, such as high thermal stability, solvent resistance, low coefficient of friction, and excellent mechanical properties. The LMPAEK being a variation of PAEK, with low melting temperature, which reduces the energy expenditure for some processes and makes them faster [20].

Cyclic Voltammetry is a technique based in the scan of the potentials on the direct and inverse directions, to follow a linear pattern. From the potentials a capacitive current is generated, which is a function of the applied potential. Thus, the Cyclic Voltammetry is the set of responses of the currents in function of the applied potentials [21–24]. From the cyclic voltammetry it is possible to have greater precision on the surface area of electrodes since this technique allows the obtaining of qualitative and quantitative parameters of the electrode. However, the use of cyclic voltammetry encounters limitations such as test time, which depends on scanning speeds, and operation control, such as disturbances in the environment, which may influence the results obtained [25, 26].

So, the present article is focused on the production and characterization of C/C composites obtained from thermoplastic composite laminates. The obtained C/C composites was evaluated and compared with those obtained through thermosetting matrix composites (phenolic resin), by means of thermal analyzes [TGA (Thermogravimetry Analysis) and DSC (Differential Scanning Calorimetry)], SEM (Scanning Electron Microscopy) and Cyclic Voltammetry.

Materials and methods

Materials

In this work, three different thermoplastic composites were used for processing carbon/carbon composites, namely: PEEK/carbon fiber (Cetex TC 1220), PEKK/carbon fiber (Cetex TC 1320) and LMPAEK/carbon fiber (Cetex 1225). All laminates were supplied by Toray Advanced Composites with the configuration [(0,90)]_{5s} and carbon fiber arrangement of 5 HS (harness satin).

Thermal properties evaluation

Thermal analyzes were performed to evaluate the thermal degradation, melting and crystallization temperatures of the materials, information that helped in the definition of the carbonization process parameters.

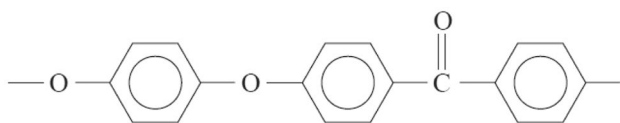


Fig. 1 Chemical structure of PEEK [14]

The thermogravimetric analysis was performed based on ASTM E1131 and E2550 standards using the equipment from SII Nanotechnology - SEIKO model TG/DTA 6200 and the following parameters were used: temperature range of 25°C to 1000°C, heating rate of 10°C.min⁻¹, an inert atmosphere with a nitrogen flow of 100mL.min⁻¹, sample weight of approximately 10mg, platinum pan and alumina as reference material.

Differential Scanning Calorimetry (DSC) analysis were performed according to ASTM D3418, and a TA Instruments equipment, model Q20 was used. DSC analyzes were performed in dual scan mode (heat-cool-heat), with a temperature range from 25 to 350°C, a heating rate of 10°C.min⁻¹, cooling rate of 5°C.min⁻¹, an inert atmosphere with nitrogen flow of 40mL.min⁻¹, aluminum hermetic pan, and a weight approximately of 10mg.

Carbon/ carbon composite processing

As previously mentioned, the C/C composites are obtained through carbonization process to remove all non-carbon elements by thermal treatments carried out at least up to 1000°C under an inert atmosphere. This is possible because the carbon withstands high temperatures, and therefore will not come out of the samples as easily, while the other elements leave the composites in the form of volatiles.

Therefore, a homemade tubular furnace with alumina-coated quartz tube was used. The process was carried out in an inert atmosphere with a nitrogen flow of 200 mL.min⁻¹, a heating rate of 3°C.min⁻¹ until 350°C and then 1°C.min⁻¹ until 1000°C, and a one-hour plateau was performed at this temperature. Hence the carbonization process lasted approximately 14 hours.

Morphological analysis

The morphological analysis was carried out to evaluate the materials morphology before and after carbonization. Therefore, the Scanning Electron Microscopy (SEM) were conducted under variable pressure or high vacuum modes, using both the secondary electrons detector and backscattered electrons one of a Zeiss EVO LS15 microscope, selected according to the sample surface conditions.

X-ray diffractometry (XRD)

The XRD test was performed to evaluate the samples crystallinity after carbonization process, thus XRD equipment from Bruker, and model D8 Advance ECO was used. The analysis was performed at room temperature with the following parameters: copper tube (Cu) with a wavelength of 1.5418 Å, scanning speed of 10°.min⁻¹, angular increment of 0.01°, region of 2θ = 10-50°, voltage of 40 kV, and 25 mA current.

Voltammetry tests

The cyclic voltammetry tests were conducted by varying the potential scan rate (2, 5, 10, 20, 30, 50 and 75 mV/s). The redox couple used was [Fe(CN)₆]⁴⁻/[Fe(CN)₆]³⁻, which is widely used because it is very sensitive to the surface conditions as well as its relationship to the structural parameters. The C/C samples, measuring (10 x 10 x 3) mm were glued on a plate welded to a copper rod with high conductivity silver paint to make the electrical contact on one side of the sample. Electrical resistance measurements were performed after assembly to ensure zero resistance to electrical contact. Then, the assembly was embedded in REDELIESE low viscosity polyester resin, delimiting a geometric area of 1.0 cm² for the C/C electrodes. This procedure makes it possible to work the carbonized composites, which are fragile, keeping exposed only the flat electrode surface (easily reproduced by mechanical polishing) that will be in contact with the electrolyte, and the copper terminal for connection to the measuring device. The C/C electrodes were sequentially polished with 220, 600, 1200 and 1500 silicon carbide silks. No surface treatment was performed on the samples before voltametric experiments. The tests were conducted in a potentiostat/galvanostat MICROQUÍMICA, model MQPG01, controlled by a program of cyclic voltammetry. The electrochemical experiments were performed using a standard three-electrode cell consisting of a platinum wire as a counter electrode, a saturated calomel electrode, Hg/Hg₂Cl₂/KCl (SCE) as the reference electrode, and as a working electrode the C/C samples. The solution was prepared by dissolving 5.0 x 10⁻³ mol/L (or 5.0 mmol/L) of K₄[Fe(CN)₆] (MERCK, p.a.) in 0.5 mol/L KCl (MERCK, p.a.) in deionized water as supporting electrolyte. The cyclic voltammetry studies were performed in solution previously deaerated by saturation with analytical nitrogen (5.0) for 15 minutes.

Results and discussion

Thermal behavior evaluation

The C/C specimens obtained from thermoplastic laminates submitted to the carbonization process presented similar characteristics to those produced from thermoset laminates, such as lightness and appearance.

The TGA analysis is normally used to study the material's thermal decomposition and is notable by the small amount of sample and the possibility to perform analyzes in a few hours. Figure 2 and Table 1 presents the results obtained through TGA analysis for the PAEK/CF, PEEK/CF and PEKK/CF, which were used to obtain the

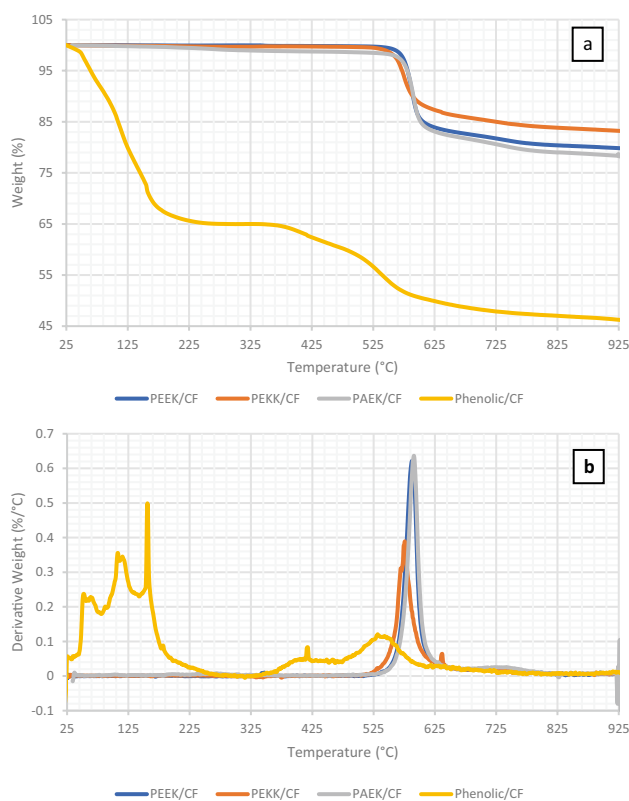


Fig. 2 TGA results for PEKK/CF, PEEK/CF, PAEK/CF and Phenolic Resin/CF

C/C composites, as well as the Phenolic Resin/CF, which has a thermoset matrix used to obtain the C/C composites (reference material).

From these results, it is observed a similar behavior of weight loss of these three thermoplastic composites, which all have at least one single weight loss between 500 and 600°C, therefore proving their high thermal stability. These three thermoplastics belong to the family of poly (ketones) thus the degradation starts from the fission of the ether and ketone bonds of the main chain. Initially, the ether and ketone groups produce a large amount of phenol and CO/CO₂ (carbon monoxide and carbon dioxide), and subsequently the fluorenone structure shows in one of the steps of the carbonization process. Thus, the main cracking products are CO and CO₂ of the fluorenone ketone group in the carbonization structure mentioned above.

The difference noted between PEKK/CF, PEEK/CF and PAEK/CF is only in the percentage of weight lost during the test, which are approximately 18%, 21% and 22% respectively. While for the phenolic resin/CF there was a final weight loss of approximately 55%, and this represents a bigger loss of material during the carbonization process for the phenolic resin/CF compared to the others.

Table 1 TGA and DSC compiled data

| | PEEK/CF | PEKK/CF | PAEK/CF | Phenolic |
|-----------------|----------|----------|-----------|----------|
| T _P | 588.06°C | 574.85°C | 590.88 °C | - |
| T _{P1} | - | - | - | 51.33°C |
| T _{P2} | - | - | - | 107.22°C |
| T _{P3} | - | - | - | 156.60°C |
| T _{P4} | - | - | - | 417.38°C |
| T _{P5} | - | - | - | 532.18°C |
| % of residue | 78% | 83% | 78% | 46 % |
| T _m | 346.23°C | 336.94°C | 307.36°C | - |
| T _C | 306.73°C | 275.79°C | 258.06°C | - |
| Cure | - | - | - | 167.46°C |

T_P corresponds to the peak temperature obtained from the derivative weigh curve in the TGA; the number next to T_P corresponds to the peaks presented in the thermal degradation of phenolic resin; T_m is the melting temperature; and T_C is the crystallization temperature

The results of TGA already indicate an advantage of the method performed with the thermoplastic matrices in relation to that done with the thermoset matrices and is noted that the thermoplastic laminates presented a higher thermal stability, since phenolic resin/CF needs five steps for its degradation, in 51, 107, 156, 417 and 532°C, while the thermoplastic matrices need just one step, that occurs in 574°C for PEKK/CF, 588°C for PEEK/CF and in 590°C for PAEK/CF. It means that the thermoset matrices have a higher complexity during the process, implying a lower heating rate throughout the carbonization process, for the output of volatiles occur correctly.

Thus, for the obtaining the C/C composites through thermoset matrices, it must be carried out slowly at a maximum of 1°C.min⁻¹ throughout the carbonization, due to the large volume of volatiles already released at the beginning of heating, and the proposed method is faster, spending less nitrogen and time, which reinforces the idea that the difference of prices that is observed would be compensated during the process of obtaining the material. In addition, the fact that thermoplastic composites exhibit lower weight loss during the carbonization process indicates that they have less pores than C/C obtained through thermosets composites. This means fewer re-impregnation steps to fill these pores, which also means an economic gain, considering that less material and hours in the furnace would be needed.

From the DSC analyses, it was possible to make the most suitable temperature and heating rate ranges throughout the carbonization process. The DSC results of the studied materials are presented in Fig. 3 and Table 1.

From the DSC analysis, it could be observed that endothermic transformations (heat gain) occurred during heating at 308°C, which represents the softening of the polymer. This temperature is important for the determination of the working temperature range in which the composite can be used, considering that from this temperature its matrix may undergo a softening, making it impossible to use. For the carbonization, it is important to know such temperature because there is a change in the behavior of the material from this point, and from this temperature the volatile exit in the composite can begin occurring, being necessary, then, a heating, so that all volatiles can exit the sample in the most appropriate way. During cooling, an exothermic (heat loss) transformation is observed at 258°C, which represents the crystallization temperature of the material. Such temperature characterizes the region in which

the crystallization in the polymer occurs more quickly and efficiently, being of important knowledge in the processing of the polymer.

Thus, considering the softening temperature as the temperature at which volatile material exit can start occurring, has been defined a heating rate of 3°C/min from ambient temperature to 350°C, and 1°C/min in the temperature range of 350 to 1000°C, the system being left at the temperature of 1000°C for approximately one hour. It should be noted that, in general, the carbonization processes performed in thermosetting matrix composites require slow heating rates (max 1°C/min) from the beginning to the end of the carbonization. In addition, more time and energy would be spent during curing of the thermosetting material, which is slow and further enhances the process, reinforcing the idea that the proposed method is more economical.

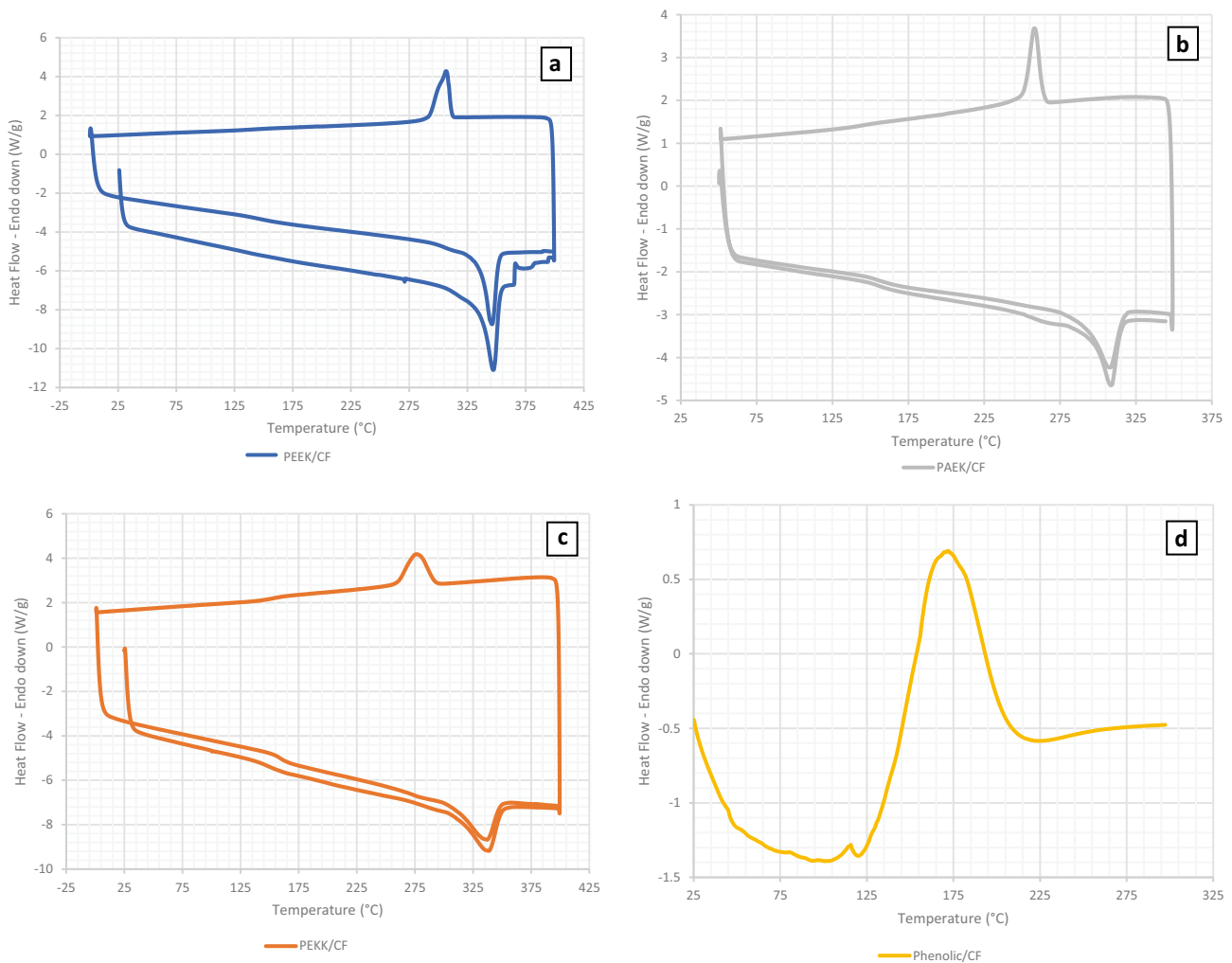
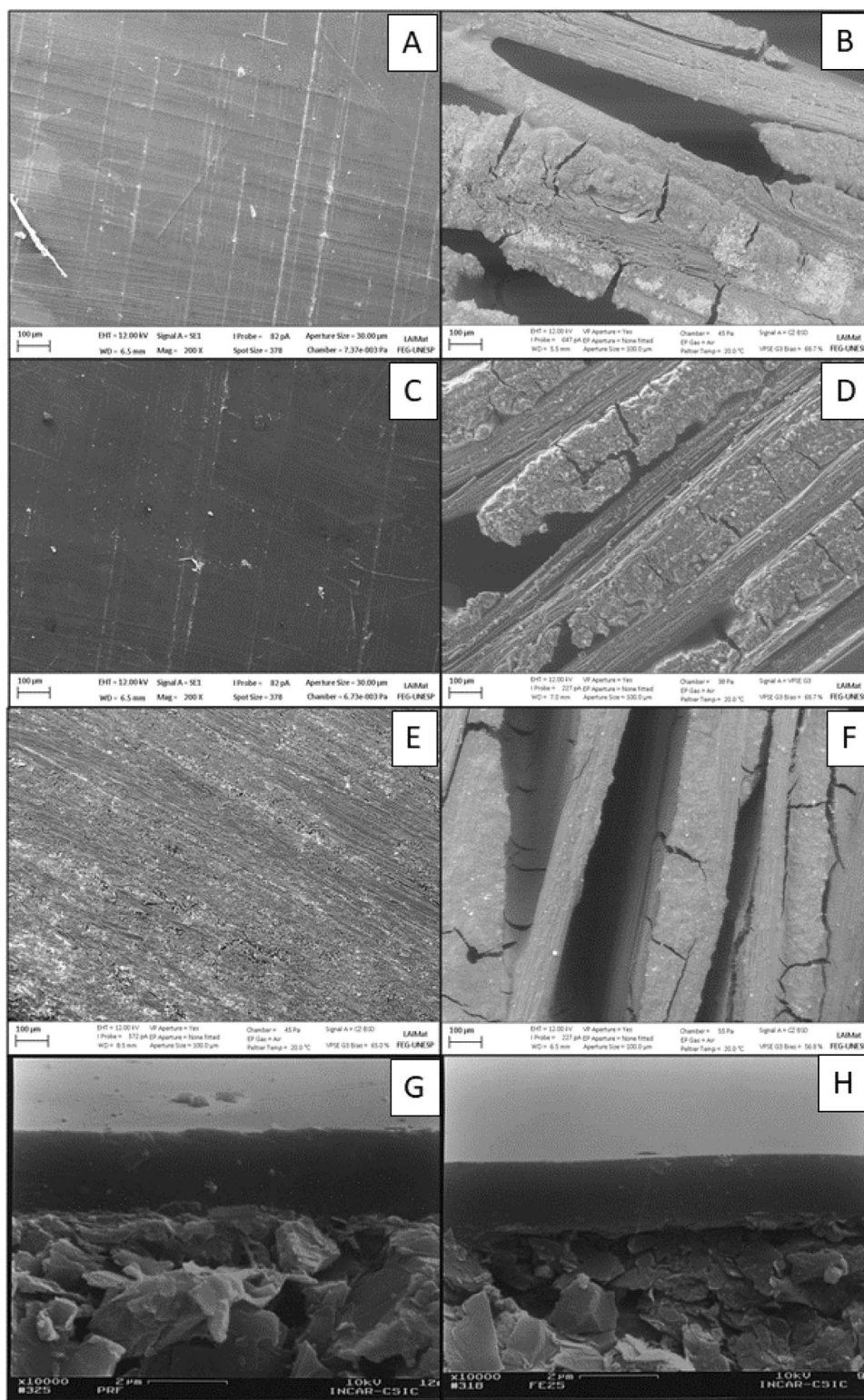


Fig. 3 DSC test performed with: (a) PEEK/CF, (b) PAEK/CF, (c) PEKK/CF and (d) Phenolic Resin

Fig. 4 Micrography of PEKK/CF (a) before and (b) after; PEEK/CF (c) before and (d) after; PAEK/CF (e) before and (f) after; and phenolic/CF (g) before and (h) after carbonization



Morphological evaluation before and after carbonization process

Evaluating the material's morphology before and after the carbonization process is important to make it possible to

better understand the process. Figure 4 shows the micrographs, with 200x magnifications, concerning about PEKK/CF, PEEK/CF, PAEK/CF, and phenolic resin/CF [27] plates before and after the carbonization process, with 10000x magnifications.

Analyzing the C/C composites morphology obtained from thermoplastic matrices is indicative that the carbonization process was carried out correctly, because there are clearly empty spaces present in the samples after the carbonization, indicating that there were exit of the other elements of the material (in this case, volatiles constituted of elements that were present in the polymeric matrix of the composite before being carbonized, like hydrogen and oxygen).

However, the morphology of the C/C composite obtained through the phenolic resin, Fig. 4g, h, has pores with different shapes and its irregular surface apparently suggests more complex pores that hindered the filling process. Despite this indicative, it would still not be possible to assure that all the elements (except for carbon) had left the material during the carbonization process, since the SEM images only show us that material has been released, but this would be a more qualitative than quantitative analysis, since a small portion of the other elements could still be present after carbonization.

In addition to morphology, another characteristic studied was the crystalline structure of the materials, so the XRD analysis was performed, and its results are show in the spectrum of Fig. 5. From the results obtained, there are two peaks, one discrete peak at approximately 12° and the other more accentuated at approximately 25°, that is, these peaks are associated with repetitive units in-plane in conjugated aromatic systems (100) and with interlayer stacking (002), respectively [28]. Comparing the spectra obtained, it can be seen that the peaks (002) have a lower intensity for the PEKK/CF and PAEK/CF samples and this characteristic is associated with a spatial confinement that prevents the formation of extended graphitic layers. And also on this analysis it can be seen that when comparing the results obtained to the XRD pattern obtained for amorphous carbon in Rajan's work [29], it looks that the samples under study have similar patterns. Therefore, suggesting that the carbonization process was carried out effectively, and only the carbon elements remains.

Electrochemical behavior of carbon/carbon composites

The cyclic voltammetry test was used to understand a possible application of C/C composites as electrodes in electrochemical systems. Figure 6 shows the cyclic voltammograms obtained for the C/C and Platinum electrodes in the scan rate range 2 to 75 mV/s. The potential sweep started at -0.1 V, in the direction of positive potentials until reaching +0.6 V, where the reversal in the direction

of the potential sweep is made until reaching the initial potential. In the anodic scan, a current peak, attributed to the oxidation of ferrocene ($[\text{Fe}(\text{CN})_6]^{4-} \rightarrow [\text{Fe}(\text{CN})_6]^{3-} + e$) is observed. After reversal in the scanning direction, a peak reduction current is observed ($[\text{Fe}(\text{CN})_6]^{3-} + e \rightarrow [\text{Fe}(\text{CN})_6]^{4-}$). For both anodic and cathodic processes, an increase in peak current values is observed with increasing scan rate. These current peaks correspond to the sum of a capacitive component (double electric layer charge) and the faradaic process, associated with the redox couple. The results also reveal that the material undergoes significant change affecting the oxidation/reduction response of $\text{K}_4\text{Fe}(\text{CN})_6$. The comparison of the voltammetric curves obtained for the C/C with the platinum electrodes shows a distortion of the cyclic voltammograms, resulting in wider current peaks and greater separation of the anodic ($E_{p,a}$) and cathodic ($E_{p,c}$), indicating a decrease in the reversibility of the process and a greater contribution of the capacitive component, in addition to a resistive component, mainly noticed at higher scan rates.

Figure 7 shows the graph of peak current density (j_p) as a function of the square root of the potential scan rate ($v^{1/2}$) for both oxidation and reduction processes of $[\text{Fe}(\text{CN})_6]^{4-}/[\text{Fe}(\text{CN})_6]^{3-}$. In all cases, there is a linear behavior of j_p vs. $v^{1/2}$, indicating that it is a diffusion-controlled process. The dependence of the peak current with $v^{1/2}$ for a reversible process is described by the Randles-Sevcik equation, which can be applied for both anodic and cathodic processes:

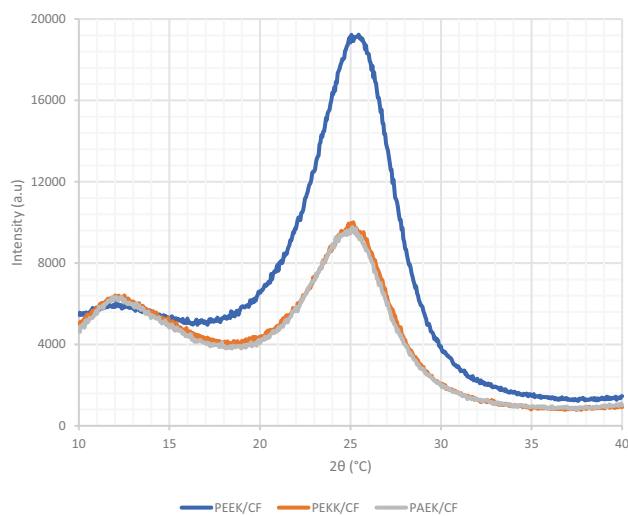


Fig. 5 XRD spectrum for samples after carbonization process

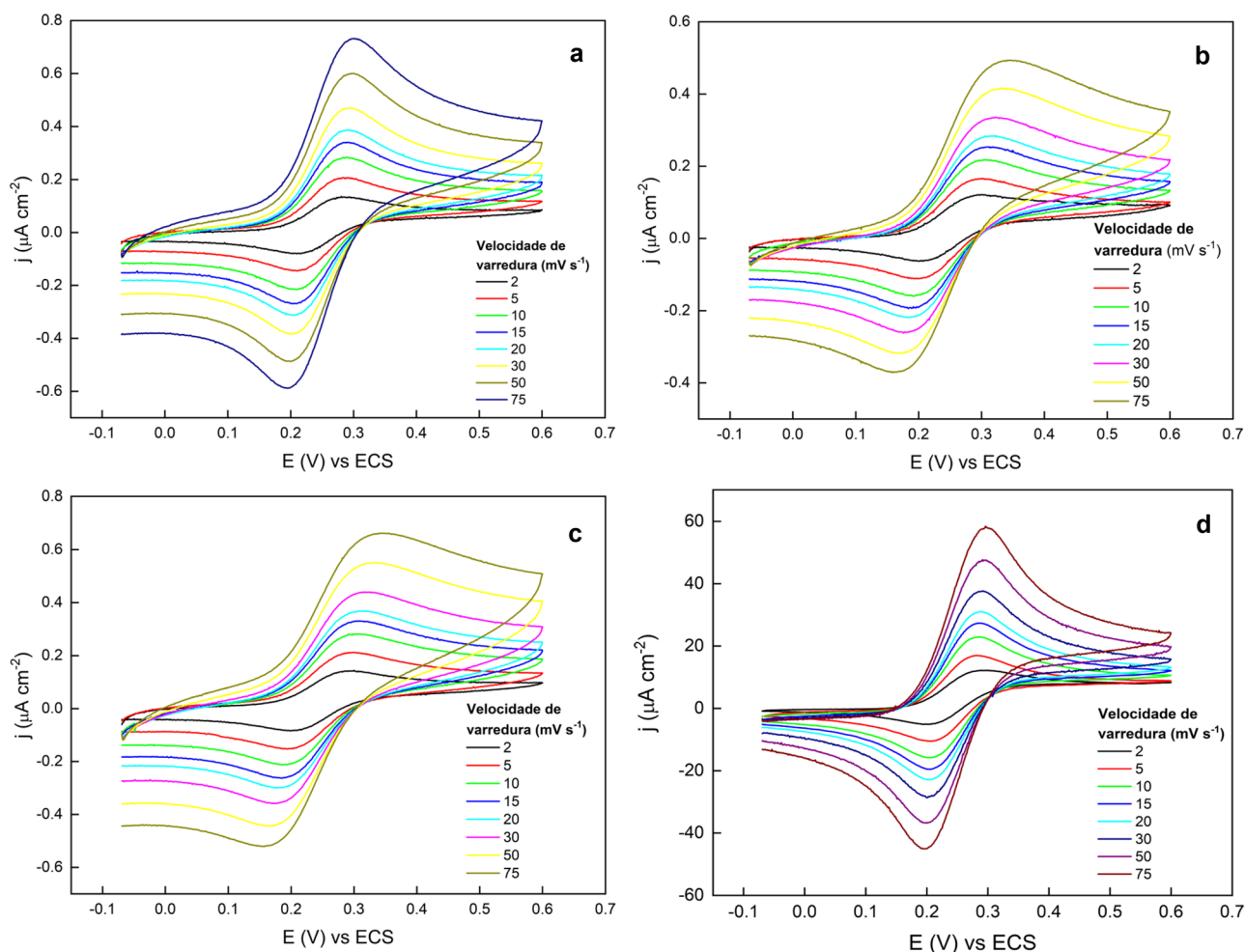


Fig. 6 Cyclic voltammograms obtained with the C/C electrodes [(a) from PEEK/CF, (b) from PEKK/CF and (c) from PAEK/CF] and with Platinum electrode (d) in 5.0×10^{-3} mol/L (or 5.0 mmol/L) $K_3Fe(CN)_6$ and 0.5 mol/L KCl solution for different scan rates

$$I_p = (2.69 \times 10^5) n^{3/2} A D^{1/2} C v^{1/2} \quad [23]$$

where I_p is the peak current (A), n is number of exchanged electrons, A is the electroactive area of electrode (cm^2), C is the concentration of the electroactive specie (mol/cm^3), D is the diffusion coefficient (cm^2/s), and v is the scan rate (V/s). According to this equation, the peak current increases with $v^{1/2}$ and is directly proportional to the concentration of the species in the solution.

A more detailed analysis of the reversibility of the oxidation/reduction process was made obtaining the value of ΔE_p - separation between the anodic ($E_{p,a}$) and cathodic ($E_{p,c}$) peak potentials at different scan rates. The comparison of the results obtained for the C/C electrodes leads us to realize that the values of ΔE_p increase as the scan rates increases, considering that the $E_{p,a}$ values are shifted to more positive potentials and $E_{p,c}$ to more negative values. In addition, comparing the ΔE_p values between the C/C electrodes with

the values obtained for the Platinum electrode, it is noted that the higher the scan rate, the greater the difference between these values of potential variation. Table 2 shows

Table 2 ΔE_p values for the C/C electrodes obtained from PEEK/CF, PEKK/CF and PAEK/CF, and for the Platinum electrode

| Scan rate (mV/s) | ΔE_p (V) | | | |
|------------------|------------------|---------|---------|--------------------|
| | PEEK/CF | PEKK/CF | PAEK/CF | Platinum electrode |
| 2 | 0.063 | 0.087 | 0.082 | 0.086 |
| 5 | 0.071 | 0.097 | 0.092 | 0.071 |
| 10 | 0.076 | 0.109 | 0.111 | 0.077 |
| 15 | 0.080 | 0.123 | 0.116 | 0.080 |
| 20 | 0.083 | 0.127 | 0.127 | 0.085 |
| 30 | 0.089 | 0.146 | 0.140 | 0.091 |
| 50 | 0.097 | 0.161 | 0.155 | 0.091 |
| 75 | 0.104 | 0.178 | 0.181 | 0.098 |

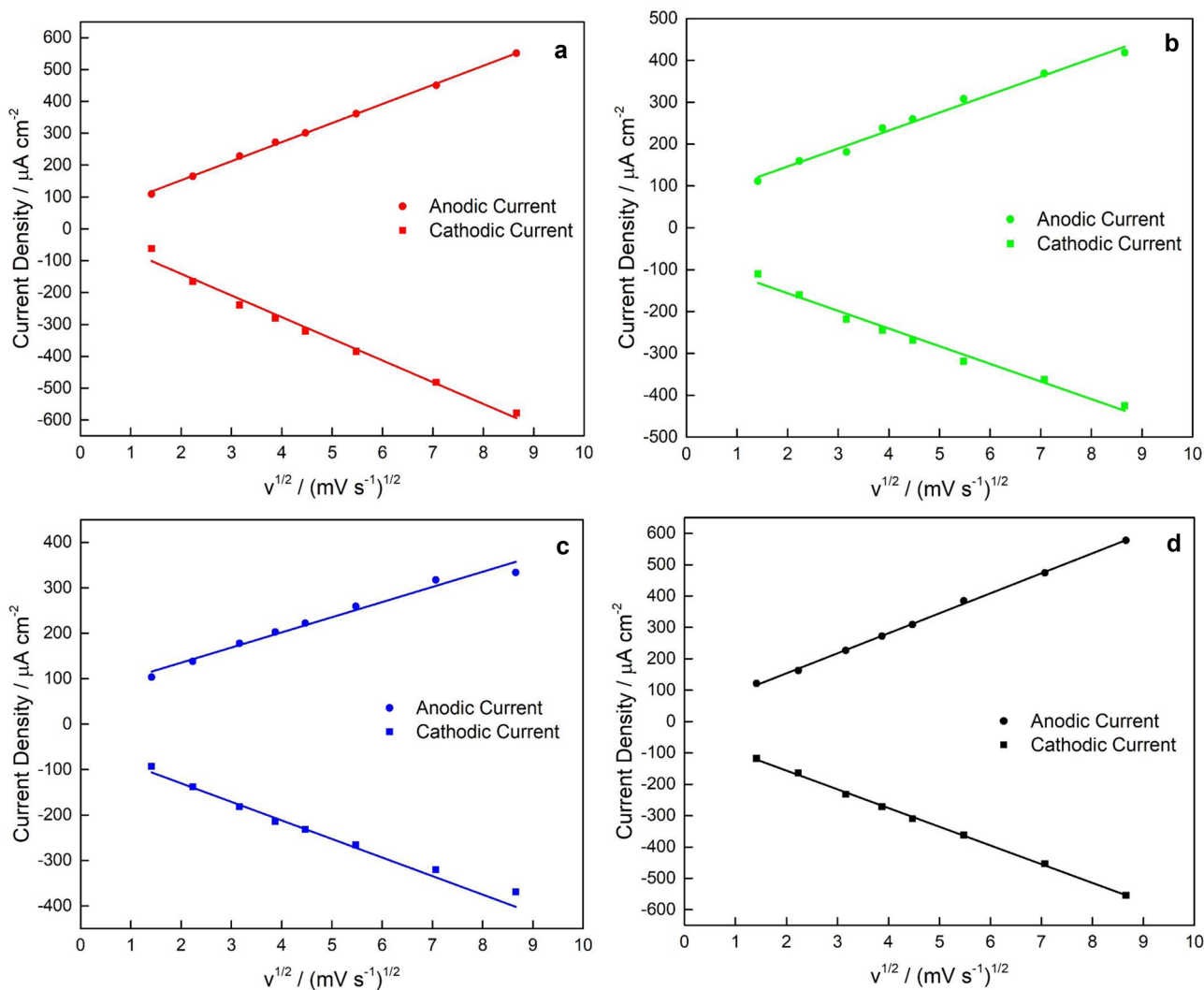


Fig. 7 Current density vs. $v^{1/2}$ for the C/C obtained from (a) PEEK/CF, (b) PAEK/CF, (c) PEKK/CF and (d) Platinum electrode in 5.0×10^{-3} mol/L (or 5.0 mmol/L) and 0.5 mol/L KCl solution

the ΔE_p values for the PEEK/CF, PEKK/CF, PAEK/CF and Platinum electrodes for different values of scan rate. The value of ΔE_p for a reversible system, involving the transfer of one-electron, as in the case of the $[\text{Fe}(\text{CN})_6]^{4-}/[\text{Fe}(\text{CN})_6]^{3-}$ couple, is 0.059 V (Kissinger, 1983). Even when a metal electrode, such as Platinum, the peak separation values are higher than expected by the theory, ranging from 0.071 V (5 mV/s) to 0.098 V (75 mV/s). The closer the behavior of the C/C electrodes to the Platinum electrode, the greater its reversibility, especially when dealing with high scan rates. Thus, it can be considered that there was a relatively similar behavior between the C/C electrodes and the Platinum electrode, which accredits them as relatively reversible.

The difference observed in the electrochemical behavior of the C/C electrode obtained through PEEK/CF and the C/C electrodes obtained through PEKK/CF and PAEK/CF can be

attributed precisely to the different materials used to obtain the C/C, which can generate different active areas in the C/C after the carbonization process, as well as different active sites, which can cause different electrochemical responses, even if the materials have the same constitution.

The electrochemical stability studies of the C/C electrodes (from PEEK/CF, from PEKK/CF and from PAEK/CF) were carried out by the application of successive scans, in the range of potentials from -0.1V to +0.6V, at a scan rate of 50 mV/s, in the 5.0×10^{-3} mol/L $[\text{K}_4(\text{CN})_6]$ in 0.5 mol/L KCl solution. All C/C electrodes showed excellent stability after 100 cycles. The potentiodynamic profiles recorded for these materials revealed a slight decrease in current for the initial scans, stabilizing after about 10 cycles. In all cases, there was a decrease of approximately 1% in the values of anodic ($j_{p,a}$) and cathodic ($j_{p,c}$) peak current density, between the first

and the hundredth cycle. No significant shift was observed in the values of anodic ($E_{p,a}$) and cathodic ($E_{p,c}$) peak potentials obtained for the respective current maximums. These results indicate a high stability of these materials in the studied electrolyte and a good reproducibility in the electrochemical response for $[\text{Fe}(\text{CN})_6]^{4-}/[\text{Fe}(\text{CN})_6]^{3-}$ couple.

Conclusions

The C/C composites produced from PEKK/CF, PEEK/CF and PAEK/CF thermoplastic matrices presented a similar characteristic as those processed from the use of thermoset matrices, such as appearance and lightness, but with faster processing and with possibility of using recycled material in the composites used as a basis for obtaining C/C laminate. In addition, processing costs were lower than for thermoset composites, due to the faster process, higher efficiency at lower carbonization loss and similar cost of PEKK/CF, PEEK/CF and PAEK/CF with the phenolic resin/CF cured and in the form of plates. Finally, considering the cyclic voltammetry tests, it can be considered that there is a relatively close behavior between the C/C electrodes and the platinum reference electrode, which allows us to consider them as good reversibility, accrediting them for such application.

Acknowledgements The authors acknowledge the financial support received from FAPESP (São Paulo Research Foundation under project 2017/16970-0 and 2018/07867-3), and CNPq (National Council for Scientific and Technological Development under project 303224/2016-9). Also, the authors acknowledge Toray Advanced Composites for the donated thermoplastic laminates.

References

1. Castanie B, Bouvet C, Ginot M (2020) Review of composite sandwich structure in aeronautic applications. *Compos Part C Open Access* 1:100004. <https://doi.org/10.1016/j.jcomc.2020.100004>
2. Kappel E (2019) Distortions of composite aerospace frames due to processing, thermal loads and trimming operations and an assessment from an assembly perspective. *Compos Struct* 220:338–346. <https://doi.org/10.1016/j.compstruct.2019.03.099>
3. Hou W, Xu X, Han X et al (2019) Multi-objective and multi-constraint design optimization for hat-shaped composite T-joints in automobiles. *Thin-Walled Struct* 143:106232. <https://doi.org/10.1016/j.tws.2019.106232>
4. Ulian G, Moro D, Valdrè G (2021) Electronic and optical properties of graphene/molybdenite bilayer composite. *Compos Struct* 255:112978. <https://doi.org/10.1016/j.compstruct.2020.112978>
5. Chen X, Wang Z, Wu J (2018) Processing and characterization of natural rubber/stearic acid-tetra-needle-like zinc oxide whiskers medical antibacterial composites. *J Polym Res* 25. <https://doi.org/10.1007/s10965-017-1433-y>
6. Li Y, Qi L, Song Y, Chao X (2017) Quantitative characterization of the carbon/carbon composites components based on video of polarized light microscope. *Microsc Res Tech* 80:644–651. <https://doi.org/10.1002/jemt.22842>
7. Buckley JD, Edie DD (1993) *Carbon-Carbon Materials and Composites*, 1st ed. Elsevier
8. Alghamdi A, Mummery P, Sheikh MA (2013) Multi-scale 3D image-based modelling of a carbon/carbon composite. *Model Simul Mater Sci Eng* 21:085014. <https://doi.org/10.1088/0965-0393/21/8/085014>
9. Jia Z, Yang C, Jiao J et al (2017) Rhein and polydimethylsiloxane functionalized carbon/carbon composites as prosthetic implants for bone repair applications. *Biomed Mater* 12:045004. <https://doi.org/10.1088/1748-605X/aa6e27>
10. Feng L, Li K-Z, Lu J-H, Qi L-H (2017) Effect of growth temperature on carbon nanotube grafting morphology and mechanical behavior of carbon fibers and carbon/carbon composites. *J Mater Sci Technol* 33:65–70. <https://doi.org/10.1016/j.jmst.2016.08.015>
11. Fitzer E (1987) The future of carbon-carbon composites. *Carbon N Y* 25:163–190. [https://doi.org/10.1016/0008-6223\(87\)90116-3](https://doi.org/10.1016/0008-6223(87)90116-3)
12. Su Y, Li K, Zhang L et al (2017) Effect of microwave heating time on bonding strength and corrosion resistance of Ca-P composite layers for carbon/carbon composites. *J Alloys Compd* 713:266–279. <https://doi.org/10.1016/j.jallcom.2017.04.189>
13. Corral EL, Loehman RE (2008) Ultra-high-temperature ceramic coatings for oxidation protection of carbon-carbon composites. *J Am Ceram Soc* 91:1495–1502. <https://doi.org/10.1111/j.1551-2916.2008.02331.x>
14. Wang T, Zhang S, Ren B et al (2020) Optimizing mechanical and thermal expansion properties of carbon/carbon composites by controlling textures. *Curr Appl Phys* 20:1171–1175. <https://doi.org/10.1016/j.cap.2020.08.002>
15. Voss H, Friedrich K (1987) On the wear behaviour of short-fibre-reinforced peek composites. *Wear* 116:1–18. [https://doi.org/10.1016/0043-1648\(87\)90262-6](https://doi.org/10.1016/0043-1648(87)90262-6)
16. Jin YS, Bian CC, Zhang ZQ et al (2017) Preparation and characterization of bio-composite PEEK/nHA. *IOP Conf Ser Mater Sci Eng* 167:012006. <https://doi.org/10.1088/1757-899X/167/1/012006>
17. Mazur RL, Botelho EC, Costa ML, Rezende MC (2008) Avaliações térmica e reológica da matriz termoplástica PEKK utilizada em compósitos aeronáuticos. *Polímeros* 18:237–243. <https://doi.org/10.1590/S0104-14282008000300009>
18. Lee SM (1992) *Handbook of Composite Reinforcements*. Wiley
19. Tadini P, Grange N, Chetehouna K et al (2017) Thermal degradation analysis of innovative PEKK-based carbon composites for high-temperature aeronautical components. *Aerosp Sci Technol* 65:106–116. <https://doi.org/10.1016/j.ast.2017.02.011>
20. Panda JN, Bijwe J, Pandey RK (2017) Comparative potential assessment of solid lubricants on the performance of poly aryl ether ketone (PAEK) composites. *Wear* 384–385:192–202. <https://doi.org/10.1016/j.wear.2016.11.044>
21. Brownson DAC, Banks CE (2014) *The Handbook of Graphene Electrochemistry*. Springer, London, London
22. Aristov N, Habekost A (2015) Cyclic voltammetry - A versatile electrochemical method investigating electron transfer processes. *World J Chem Educ* 3:115–119
23. Kissinger PT, Heineman WR (1983) Cyclic voltammetry. *J Chem Educ* 60:702. <https://doi.org/10.1021/ed060p702>
24. Gooding JJ (2005) Nanostructuring electrodes with carbon nanotubes: A review on electrochemistry and applications for sensing. *Electrochim Acta* 50:3049–3060. <https://doi.org/10.1016/j.electacta.2004.08.052>

25. Calixto CMF, Mendes RK, de Oliveira AC et al (2007) Development of graphite-polymer composites as electrode materials. *Mater Res* 10:109–114. <https://doi.org/10.1590/S1516-14392007000200003>
26. de Souza LL, Forbicini CD (2014) Uso da voltametria cíclica e da espectroscopia de impedância eletroquímica na determinação da área superficial ativa de eletrodos modificados à base de carbono. *Eclética Química* 39:49–67
27. Fuertes AB, Centeno TA (1999) Preparation of supported carbon molecular sieve membranes. *Carbon NY* 37:679–684. [https://doi.org/10.1016/S0008-6223\(98\)00244-9](https://doi.org/10.1016/S0008-6223(98)00244-9)
28. Hao M, Li Y, Gao L et al (2020) In-situ hard template synthesis of mesoporous carbon/graphite carbon nitride (C/CN-T-x) composites with high photocatalytic activities under visible light irradiation. *Solid State Sci* 109:106428. <https://doi.org/10.1016/j.solidstatesciences.2020.106428>
29. Rajan AS, Sampath S, Shukla AK (2014) An in situ carbon-grafted alkaline iron electrode for iron-based accumulators. *Energy Environ Sci* 7:1110–1116. <https://doi.org/10.1039/c3ee42783h>

Publisher's Note Springer Nature remains neutral with regard to jurisdictional claims in published maps and institutional affiliations.